

Dynamics of Solvated Chloride Inhibition by Nanoparticle Treated Concrete

Harish Venkateshaiah¹, Jinko Kanno², Nicholas Richardson², James Phillips², Kunal Kupwade-Patil³, Henry E. Cardenas³ and Daniela S. Mainardi¹

¹Chemical Engineering Program/ Institute for Micromanufacturing, Louisiana Tech University, Ruston, LA 71272

²Mathematics Program, Louisiana Tech University

³Mechanical Engineering Program, Louisiana Tech University

Abstract

Corrosion of steel reinforcement in concrete is caused largely by ingress of chloride ions from deicing salts and coastal marine environments. Electrokinetic nanoparticle treatment concurrent with electrochemical chloride extraction have been employed to minimize chloride attack and reinstate the passivity of embedded steel. Additionally, pozzolanic nanoparticles such as aluminum- and silicon-containing materials can be injected into concrete pores using externally applied electric fields in order to reduce permeability of chloride ions into concrete. We present results of computational simulations used to investigate dynamics of solvated chloride anion (Cl^-) through a tricalcium silicate nanopore in the presence of alumina (Al_2O_3) and silica (SiO_2) nanoparticles that form the main binder phase of Portland cement. First, equilibrium properties of $\text{Cl}^-(\text{H}_2\text{O})$ system are explored, using Density Functional Theory with-localized GGA exchange correlation functional of PW91. Microsolvation conformers are thus obtained as a gradual approach to bulk solvation structures. Cl^- atomic size is explored using radial distribution functions (RDF). Molecular Dynamics in the canonical ensemble is used to obtain coefficient of diffusion of solvated Cl^- at 25 °C. Diffusivity calculated from the variation of the mean square displacement of the chloride ions with time show considerable differences depending on their position with respect to nanoparticles. Increase in ion size after solvation and its diffusivity obtained implicate both solvation structure and alumina-silica nanoparticles as controlling factors for Cl^- dynamics in aqueous systems inside concrete pores.

I. Introduction

In the US alone, research programs are established by the Federal Highway Administration for corrosion protection in concrete bridges at high priority to develop economical modes of corrosion containment. Concrete is a composite material that consists essentially of binding medium within which are embedded particles of aggregate that form the porous structure of concrete. Corrosion of reinforcement steel is estimated to have rendered 29.6% of concrete structures deficient or functionally obsolete, as per the US Federal Highway Administration in 1996. Highway bridge repairs alone afflicted an enormous annual direct cost of \$8.3 billions [1]. Chloride-induced corrosion is auto-catalytic in nature. The aggressive anion penetrates the porous cementitious material triggering electrochemical reactions corroding the reinforcement [2,3]. Recent application of electrokinetic nanoparticle treatment is known to reduce the permeability, and therefore ionic transport [4]. Adequate porosity reduction was attained to improve the durability of cementitious material considerably. Using electric field, reactive pore

blocking chemicals were driven into the saturated concrete pores. The nanoparticles react with cementitious material in presence of moisture to form a main binder phase in Portland cement [5].

Uncertainty is involved with material properties, structure geometry and dimensions, as well as with analytical models of chloride penetration into concrete and onset of reinforcement corrosion though probabilistic models have been developed to understand the extent of damage done [6,7]. The present work investigates diffusion of the chloride anion in the presence of water. Molecular modeling is used to simulate the nanosystem of concrete pore with nanoparticles, analogous to experimental [5] and analytical models [8] developed already. The diffusivity of chloride ions is determined by the MSD method after conducting Molecular Dynamics calculations.

II. Simulation Methods

Solvation of Chloride Anion (Cl⁻) Using Density Functional Theory:

The DMOL³ module of the Material Studio program developed by Accelrys, Inc. has been used to carry out Density Functional Theory (DFT) calculations, to obtain a local minima conformer representative of solvated Cl⁻. Vibrational frequencies of the model and the charge population are computed for the geometry optimization step. A customized geometry optimization calculation was employed with a non-localized Generalized Gradient Approach (GGA) exchange correlation functional of Perdew and Wang (PW91). Ground spin state was determined by setting up spin-unrestricted calculation without using symmetry information. Total charge of the water-anion system is set to -1e (charge on anion). With an explicit solvent model, all electrons in the system are included in the calculation. Double Numerical plus polarization (DNP) basis set was used since it includes polarization *p*-function on all hydrogen atoms in water system involving hydrogen bonding. DNP essentially includes one atomic orbital for each occupied atomic orbital, a second set of valence atomic orbitals and a polarization *d*-function on all non-hydrogen atoms. Electrostatic potential-derived Merz-Kollman charges of 0.393 and -0.787 e are applied to the hydrogen atoms and oxygen atom of a single water molecule, respectively.

Tricalcium Silicate (C₃S) Nanopore Using Molecular Mechanics and Dynamics:

Forcite module of the Material Studio program developed by Accelrys, Inc. has been used for Molecular Mechanics (MM) geometry optimization calculations. C₃S unit cell was used to model a concrete nanopore by building a *supercell* of required dimensions. Cylindrical nanopore of about 6 nm diameter and 8 nm height was built. Constraint to atomic motions was applied on parts of the cylinder that do not come in contact with the nanosystem inside the pore for ease of computation. XYZ components of such atomic positions were held constant in the Cartesian space. Geometry minimization calculation was done using the Smart Algorithm, which is a cascade of steepest descent, conjugate gradient, quasi-Newton, and ABNR method. Maximum energy change of ~0.02 kcal/mol was tested as convergence threshold, discounting the force, stress, and displacement. *Universal* forcefield was used to describe interatomic bonded and non-bonded interactions. The non-bond terms in the structure were evaluated by *atom-based* summation method. The electrostatic and van der Waals' forces between all the atoms in the structure participate in the summation. *Normal* convergence was achieved for maximum iterations set to 10,000 optimization cycles. The alumina and silica nanoparticles were modeled

by repeating the above procedure, with no constraints applied to motion of its atoms. Diameters of 0.5 nm for alumina and 2 nm for silica were modeled using respective *supercell*. The models of nanopore and nanoparticles were converted to non-periodic structures. An external electrode of silver (Ag) with adequate positive charge was placed at one end of the cylinder to generate sufficient potential to electrostatically attract negatively charged free Cl^- . Concrete cylinder with alumina-silica nanoparticles, and external electrode was minimized using the Forcite Geometry Optimization calculations setup for the concrete pore previously.

Further Molecular dynamics (MD) calculations were used in this work. MD integrates Newton's law of motion for all atoms in the molecular system with statistical mechanics for the prediction of transport properties [9]. Fundamental transfer property of ions such as diffusivity needs to be evaluated at confined regions to understand its dynamics at the interface. Lower number of hydrogen bonds and reduced density in this region causes interfacial water molecules to translate and rotate at a faster rate than in bulk molecules. Dynamic properties of interfacial water molecules are less affected by ion concentration unlike the bulk water molecules. Hence, interfacial water molecules can be expected to preferentially solvate Cl^- since the solvation free energy depends on the relative location of solute ions at the interface. Hence, MD is effective in providing reasonable free energy data for even systems with many energy minima separated by energy barriers [10].

Mechanism of ionic transfer and free energy of ion across liquid interfaces provides insight on equilibrium properties and dynamics of ions. Understanding the solvation and adsorption of ions in aqueous interfaces is essential in modeling and controlling chemical reactivity [10]. Dynamics of the solvated Cl^- in concrete pore system are studied using MD. The calculations setup for MD has been discussed in detail in further sections.

III. RESULTS AND DISCUSSION

A. Static Properties and Energetics

This section presents the results of simulations carried out to prepare input models for the subsequent dynamics study of Cl^- in a concrete pore system along with alumina-silica nanoparticles.

1. Solvated chloride ion

The chloride anion-water $[\text{Cl}(\text{H}_2\text{O})_n]$ minimum energy structure was obtained from DFT calculations for $n=1$ to 13 and 16 to 25. These geometries correspond to relative minimum on the potential energy surface. The structures are reported as minima for $\text{Cl}(\text{H}_2\text{O})$. Though solvation can occur with 6 water molecules [11], models of $n=1$ to 6 were found to be surface anions [12].

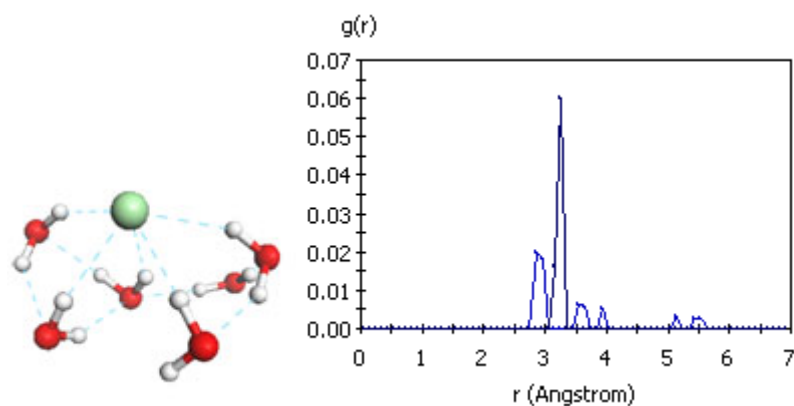


Figure 1: Microsolvation structure $\text{Cl}^-(\text{H}_2\text{O})_{n=6}$ with radial distribution function of O- Cl^-

The solvation clusters represent a stationary point on the energy surface where forces on all atoms are zero [13]. The relative energies of such ground states corresponding to stable structure are reported in table 1. Ion position got more interior with higher water molecules. Anion completely solvated is expected to lie within the liquid water network or surrounded by the water molecules [12,14]. Internal solvation was observed for $n > 17$ as shown in figure 2, and simulation was continued till $n = 25$ to confirm this transformation from surface to internal solvation [15]. Table 1 also reports the relative ground state energy per water molecule of each model.

Table 1: Electronic energies of ground states for $\text{Cl}^-(\text{H}_2\text{O})_n$ for $n=1$ to 13 and 16 to 25

No. of Water Molecules per Cl^-	Total Electronic Energy (10^5kcal/mol)	Electronic Energy per water molecule (10^5kcal/mol)
1	-3.37	-3.37
2	-3.85	-1.92
3	-4.33	-1.44
4	-4.81	-1.20
5	-5.29	-1.06
6	-5.77	-0.96
7	-6.25	-0.89
8	-6.73	-0.84
9	-7.21	-0.80
10	-7.69	-0.77
11	-8.17	-0.74
12	-8.65	-0.72
13	-9.13	-0.70
16	-10.57	-0.66
17	-11.04	-0.65
18	-11.52	-0.64
19	-12.00	-0.63
20	-12.48	-0.62
21	-12.96	-0.62
22	-13.44	-0.61
23	-13.92	-0.61
24	-14.40	-0.60
25	-14.88	-0.60

Vibrational frequencies were checked to ensure ground state conformations. At least 3 minima conformers were obtained for each combination of $\text{Cl}^-(\text{H}_2\text{O})_n$ for $n=1$ to 13 and 16 to 25, to explore different local minimum configurations. Large reorganization is observed within the hydrogen-bonded (H-bond) water network and the anion seems to travel to the surface of the shell. The smaller clusters continue to show clearly the surface solvation of anions for up to $n<18$. Larger clusters show an indication of liquid water hydration. The anion is completely surrounded by water molecules only after $n=18$, which gives a good scale [16] for cluster size to be used further in our MD simulations, since $\text{Cl}^-(\text{H}_2\text{O})_{n=25}$ binds its excess electron more strongly than with less number of water molecules (figure 3). Results show strong H-bonding between Cl^- and hydrogen atoms of water (O-H— Cl^-) and between the individual water molecules (O-H—O). Different minima for same n (number of water molecules) showed the lowest energy configuration to have lesser number of O-H— Cl^- bonds. This indicated more stable structures for clusters with more interwater H-bonding for a particular n [11].

Radial distribution function:

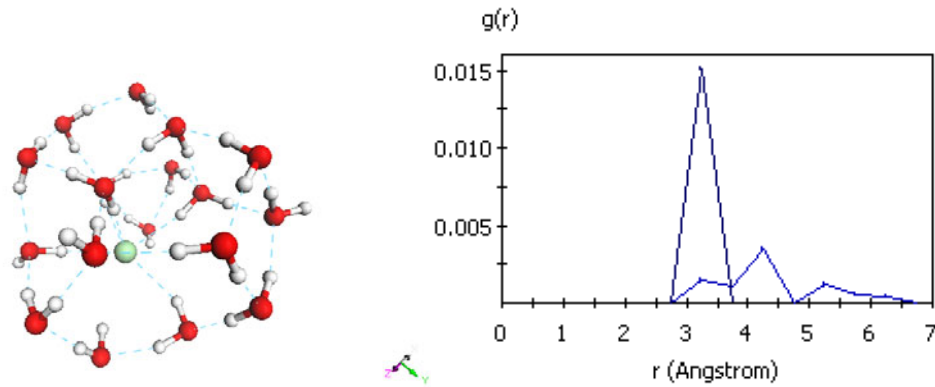


Figure 2: Internal solvation structure $\text{Cl}^-(\text{H}_2\text{O})_{n=18}$ with radial distribution function of O- Cl^-

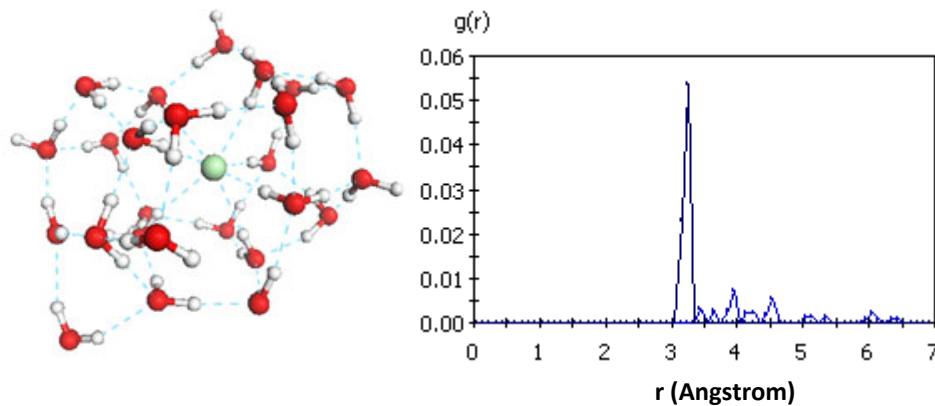


Figure 3: Completely solvation structure $\text{Cl}^-(\text{H}_2\text{O})_{n=25}$ with radial distribution function of O- Cl^-

The radial distribution functions (RDFs) of Cl^- is shown in figures 1, 2 and 3 for different $n=6$, 18 and 25. The structural influence of Cl^- is expected to extend up to a second solvation shell [17]. The plots of distribution function for radial distance for O- Cl^- distance indicates first hydration shell size of ~ 0.33 to 0.34 nm for system of 6, 18 and 25 water molecules at the highest peaks of respective plots. Figure 1 shows a first peak at ~ 0.28 nm and a second high peak at 0.33 nm due to surface solvated position of Cl^- in the shell. There is no peak at 0.28 nm in figures 2 and 3 since the Cl^- is more surrounded by water molecules. X-ray and neutron diffraction measurements are known to show hydration of one Cl^- with 6 water molecules [11]. Using the atomic radius of oxygen atom of 0.152 nm [8], we observe that the size of the solvated anion is higher than its atomic radius of free Cl^- .

2. Alumina-silica Nanoparticles and Concrete Nanopore

Chloride ion penetration in concrete was investigated experimentally [5] for Portland cement concrete cylinder of 3in diameter and 6in length. 2 nm alumina coated over 20 nm silica composites reduced the porosity of concrete by forming a binding phase.

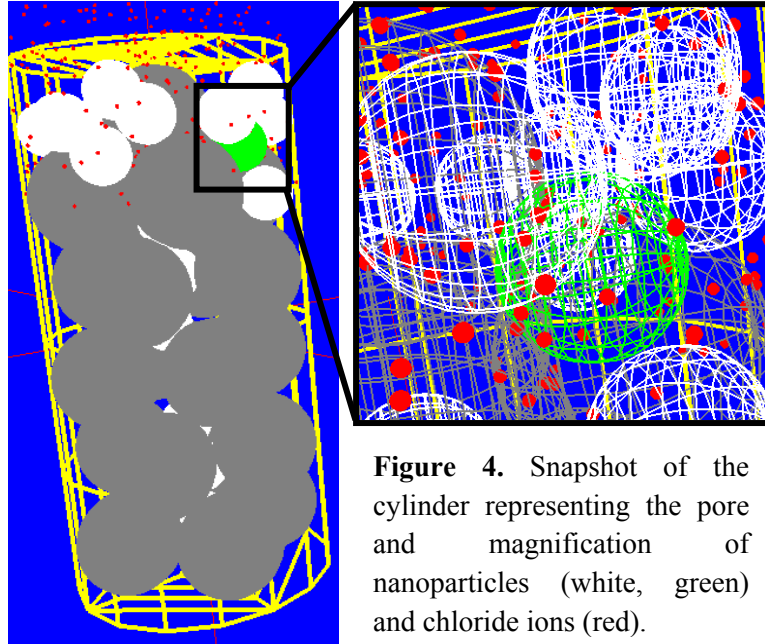


Figure 4. Snapshot of the cylinder representing the pore and magnification of nanoparticles (white, green) and chloride ions (red).

The concrete pore with the nanoparticles and solvated ion were also modeled analytically. The cylinder and spheres representing the system is shown in figure 4. Stacking and packing assembly methods were used such that each particle stays inside the cylinder and also interacts with each other to nearly represent the actual system. Porosity reduction of ~57% was achieved after the model was tested for different combinations of nanoparticles size. Considerable porosity reduction was obtained for a diameter combination of 1:4 and 1:5 [8].

In the present work the sizes of nanoparticles are scaled down for computational ease still maintaining the size ratio. The experimental work showed that particles aggregate with a positive charge making it possible to drive them all the way to the steel reinforcement inside concrete. The alumina on contact with steel adheres to its surface to protect steel from dropping in pH to remain passivated for longer duration [4]. Silica suspension is known to have higher buffer capacity than alumina, and increases the pH of the medium. Though alumina does not aggregate in suspension, on introduction of silica, it forms heteroaggregates owing to opposite charges. Silica suspension is known to have higher buffer capacity than alumina, and increases the pH of the medium. Figure 5 shows the structure optimized to use in MD runs. The nanoparticles were stacked inside the cylinder to cover most of the through space, though not to the extent as in the analytical stacking. It can be observed that the inner surface of the concrete cylinder reacts with few alumina particles adhering to its surface. The silica adsorption is not visually evident due to tight packing. In presence of water the silica is expected to form a binding phase C-S-H.

3. Mean Square Displacement of Chlorides Using Molecular Dynamics (MD)

Forcite module of the Material Studio program developed by Accelrys, Inc. has been used for Molecular Dynamics (MD) calculations to investigate the dynamics of the Cl^- in modeled nanosystem. Four clusters of solvated chloride ion (4 Cl^- ions-100 water molecules) were introduced into the concrete pore system optimized using Molecular Mechanics. The *canonical ensemble* of NVT (number of atoms, system volume and temperature remains constant) for the thermodynamic calculations for atoms in the non-periodic system. *Velocity initialization* for atoms in the system was set using random values with a temperature-dependent Gaussian

distribution. A default time step of 1.0 fs is selected with *number of steps* as 5000. These two factors determine the simulation time. A *frame output* of 50 is selected for frequency at which the simulation frame is to be written to the trajectory file. The task parameters controlling accuracy and speed of the MD calculation is set at *coarse* level to better simulation speed, without compromising accuracy of calculation, which would be possible in case of a periodic structure. *Universal* forcefield is chosen to approximate the PES using ‘current’ system charges. The summation methods for the non-bond interactions- electrostatic and van der Waals, is set to atom based since no groups are defined for this non-periodic system. The dynamics simulation output is then used to analyze the mean square displacement of the chloride ions defined as a distinctive set. From the generated data (a plot of mean square displacement of chloride ions vs. time) the slope of the curve should be equal to $2dD$, which gives the final value of chloride diffusivity [9].

Dynamics of solvated chloride- Molecular dynamics

Continuous and discrete models have been adopted for the simulation methods to study ionic mobility. The geometry minimized system after molecular mechanics (figure 5) is used for dynamics run input. The dynamics simulation was conducted at 25 °C and pH 7. The electrostatic forces due to externally applied electric field cause the negative chloride to travel across the nanoparticles. The dynamics of chloride ions with respect to the nanoparticles is studied by fixing the surrounding system of concrete matrix and opposite charge electrode. Only the internal surface of concrete cylinder is found to aggregate with the nanoparticle; which is comparable to the formation of binding phase on cement. The chlorides are found to break out of the solvation shell and travel across the nanoparticles. The majority of system energy is observed to be from bond, angle, torsion, and inversion interactions, as compared to the non-bond energy. System potential energy reduction from initial configuration is lesser when compared to the kinetic energy change. The temperature convergence is observed to be satisfactory with low standard deviation and the average reading being close to required temperature.

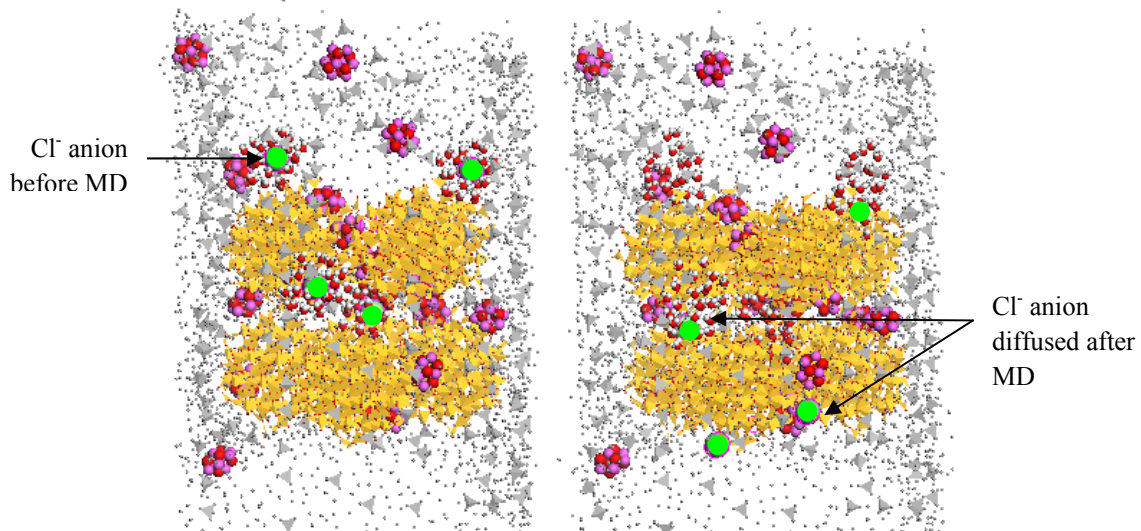


Figure 5: Concrete pore (grey) model with solvated Cl⁻ (green) and Al₂O₃ (pink)/SiO₂ (yellow) nanoparticles.

The MD simulation output is shown in figure 5. Initially, the 4 solvated chloride ions were seen within the water network. The cylinder model in figure 6 is ~ 8 nm in height. Assuming the bottom of cylinder to be '0 nm' and measuring up to '8 nm' at the top, the diffusion is observed from 8 to 0 nm (top of cylinder to bottom), since the applied external field is a positive charge of $+1e$ or 1.6×10^{-19} coulombs per Ag atom in the electrode, at the 0 nm. The initial position of the 4 anions prior to MD is reported in table 2 with respect position along axial length of the cylinder, starting with anion *A* being the farthest and *D* the closest.

Table 2: Diffusivity of each anion compared to distance from externally applied electric field.

Cl ⁻	Initial position (Distance measured from 0 to 8 nm)	Individual diffusivity, $D * 10^{-3}$ in cm ² /s
D_A	6.75	1.55
D_B	6.53	5.06
D_C	4.34	2.73
D_D	3.94	3.82

The coefficient of diffusion of each ion calculated from mean square displacement (MSD) of ions is reported in table 2. *A* was placed the farthest across the nanoparticles and showed lowest diffusivity among the 4 ions. On the other hand *B* placed at similar distance showed maximum diffusivity $5.06 \text{ cm}^2/\text{s}$. This indicates *B* traversed the cylinder along a path with voids, while path of *A* was blocked by the alumina-silica aggregates.

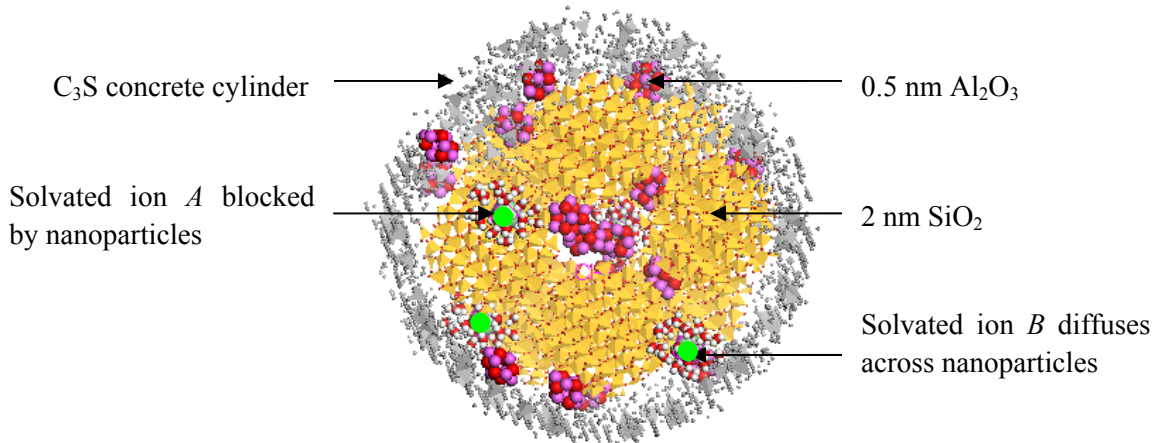


Figure 6: Top view of cylinder highlighting position of Cl⁻ ions (A & B)

The free chlorides diffuse farther across as compared to the solvated chloride. The solvated anions are defined as unique set in the simulation output trajectory and the dynamics is quantified by mean displacement method using the Einstein's law. The calculation of diffusivity *D* of all 4 chloride ions is shown below along with the MSD profile versus time.

The slope of the linear profile of the curve is $154.9 \text{ \AA}^2/\text{ps}$. Using Einstein's equation:

$r^2(t) = 2dDt$, where D = diffusivity and $d=3$ for 3-D systems, the diffusion coefficient of chloride ions is $D = 2.58 \times 10^{-3} \text{ cm}^2/\text{s}$.

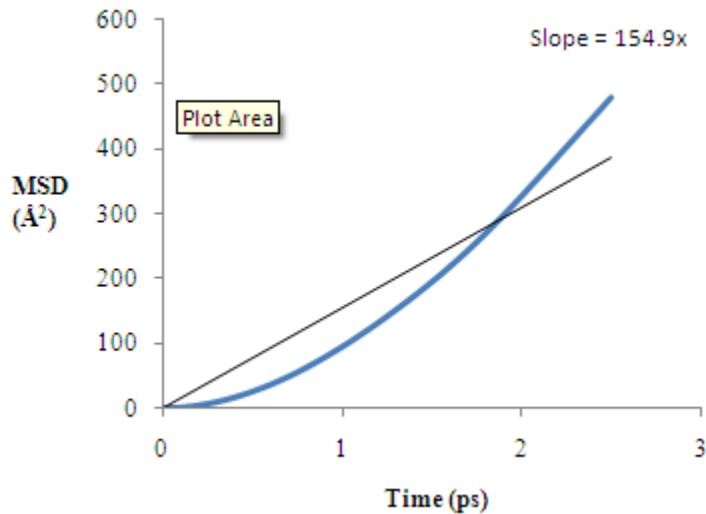


Figure 7: Mean square displacement of solvated Cl^- anions with time

IV. CONCLUSION

Solvation provided Cl^- atomic radius slight increase for $n=2$ to 25. Larger hydration shells are to be explored to confirm considerable size increase. Size ratio of the nanoparticles modeled (1:5) was in agreement with the analytical model that attained highest porosity reduction. Ionic diffusivity for anions A and B was considerably high; which indicates that the model needs to be investigated with better packing of the nanoparticles inside the pore and different electric field strengths.

References

1. Klieger, P; Lamond, J. F. "Significance of Tests and Properties of Concrete and Concrete-Making Materials," *ASTM International*, 1994.
2. Schweitzer, P. A. "Corrosion Engineering Handbook," *Marcel Dekker*, 1996.
3. Amleh, L.; Mirza, M. S. "Corrosion Response of Decommissioned Deteriorated Bridge Deck," *Journal of Performance of Constructed Facilities*, 2004, 18 (4), 185-194.
4. Cardenas, H. E.; Struble, L. J. "Electrokinetic Nanoparticle Treatment of Hardened Cement Paste for Reduction of Permeability," *Journal of Materials in Civil Engineering* 2006, 554-560.

5. Cardenas, H. E.; Kupwade-Patil, K. V. "Corrosion Mitigation in Concrete Using Electro-Kinetic Injection of Reactive Composite Nanoparticles," *Journal of the American Concrete Institute*, Submitted January **2007**.
6. Mears, R. B.; Brown, R.H. "Corrosion Probability," *Industrial and Engineering Chemistry*, October **1937**, 29 (10); 1087-1091.
7. Lounis, Z. "Probabilistic Modeling of Chloride Contamination and Corrosion of Concrete Bridge Structures," *IEEE Computer Society* **2003**, Proceedings of the Fourth International Symposium on Uncertainty Modeling and Analysis.
8. Kanno, J.; Richardson, N.; Phillips, J.; Kupwade-Patil K.; Mainardi, D.S.; Cardenas H.E. "Modeling and Simulation of Electromutagenic Processes for Multiscale Modification of Concrete" *Proceeding paper of the 12th World Multi-Conference on Systemics, Cybernetics and Informatics: WMSCI 2008*. June 29th - July 2nd, **2008** – Orlando, Florida, USA.
9. Leach, A. R. "Molecular Modeling- Principles and Application," *Prentice Hall*, 2nd Edition **2001**.
10. Chang, T; Dang, L. "Recent Advances in Molecular Simulations of Ion Solvation at Liquid Interfaces," *Chem. Rev.* **2006**, 106, 1305-1322.
11. Pathak, A. K.; Mukherjee, T.; Maity, D. K. "Microhydration Shell Structure in $\text{Cl}_2^- \cdot n\text{H}_2\text{O}$ clusters: A Theoretical Study," *J. Chem. Phys.* **2006**, 125, 074309.
12. Simons, J. "Molecular Anions," *J. Phys. Chem. A.* **2008**, 112, 6401-6511.
13. Reichardt, C. "Solvent and Solvent Effects: An Introduction," *Organic Process Research and Development* **2007**, 11, 105-103.
14. Christopher, H.; Holbrey, J. D.; Nieuwenhuyzen, M.; Youngs, T. G. A. "Structure and Solvation in Ionic Liquids," *Acc. Chem. Res.* **2007**, 40, 1146–1155.
15. Kemp, D. D.; Gordon, M. S. "Theoretical Study of the Solvation of Fluorine and Chlorine Anions by Water", *J. Phys. Chem.* **2005**, 109, 7688-7699.
16. Daguene, C.; Dyson, P. J. "A Metallacage Encapsulating Chloride as a Probe for a Solvation Scale in Ionic Liquids," *Inorg. Chem.* **2007**, 46, 403-408.
17. Heuft, J. M.; Meijer, E. J. "Density Functional Theory based Molecular-Dynamics Study of Aqueous Chloride Solvation," *J. Chem. Phys.* **2003**, 119(22), 11788-11791.
18. Cerbelaud, M.; Videcoq, A.; Abelard, P.; Pagnoux, C.; Rossignol, F.; Ferrando, R. "Heteroaggregation between Al_2O_3 Submicrometer Particles and SiO_2 Nanoparticles: Experiment and Simulation," *Langmuir*, 2008, 24, 3001-3008.
19. Bizzarri, A. R.; Cannistraro, S. "Molecular Dynamics of Water at the Protein-Solvent Interface," *J. Phys. Chem. B.* **2002**, 106(26), 6617-6633.
20. Lee, S. H.; Rasaiah, J. C. "Molecular Dynamics Simulation of Ion Mobility.2. Alkali Metal and Halide Ions Using the SPC/E Model for Water at 25 deg C," *J. Phys. Chem.* **1996**, 100, 1420-1425.